

Distribution of copy number alterations and impact of chromosome arm call thresholds for meningioma

Received: 24 February 2024

Accepted: 3 June 2025

Published online: 02 July 2025



Ruchit V. Patel¹, Hia S. Ghosh¹, David M. Meredith², Scott Ryall², Elizabeth B. Claus^{1,3}, Rameen Beroukhi⁴, Azra H. Ligon², Sandro Santagata² & Wenya Linda Bi¹✉

Chromosome-arm copy number alterations (CNAs) are an important component of cancer molecular classifiers. CNAs are often translated into binary chromosome arm calls (arm gain/loss) using an arm call threshold before integration into classification schemes. However, substantial variability exists in thresholds used to define arm calls from CNA data. Here, we analyze 1042 meningiomas with whole-genome microarray data and 13 meningiomas with multifocal sampling to characterize how CNA thresholds influence molecular classification and prognostication. Changing arm call thresholds shifts the association of chromosomal arm calls with meningioma recurrence in an arm-dependent manner and upgrades 21.5% of cases from low-grade to high-grade in a molecularly Integrated Grade (IG) scheme. The impact of threshold differences in IG prediction of recurrence is most evident amongst intermediate grade (IG-2) tumors and CNA call thresholds approaching whole-chromosome arm length (>95%). The designation of chromosome loss or gain remains stable across a majority of thresholds, although this varies in a chromosome-dependent manner. CNAs fluctuate among paired primary-recurrent tumors, mostly growing on recurrence, but cluster in discrete sizes within a tumor. Appreciation of the impact of chromosome arm call thresholds can help ensure robustness of molecular classification paradigms.

The introduction of molecular profiling has transformed our ability to classify and predict the outcome of patients with both solid and liquid cancers¹. Molecular classification schemes incorporate information on genome copy number alterations (CNAs), structural variation, gene mutations, and/or DNA methylation in a tumor-dependent manner^{2–7}.

CNAs reflect gains and losses of DNA across the genome^{8,9}, which can occur on any chromosome arm and vary considerably in size^{10,11}. Rather than using the precise chromosomal location and/or size of CNAs, molecular classifiers commonly convert this

information into a binary chromosome arm call, also known as a broad gain or loss. CNAs are translated to chromosome arm calls by comparing the size of a CNA to an arm call threshold, defined by the research investigator or institution. When the size of the CNA exceeds this threshold, a chromosome arm call is generated. For example, with a threshold of 50%, if the size of a copy number gain/loss exceeds 50% of the arm, an arm gain/loss call is generated, while if the CNA affects <50% of the chromosome arm, no arm call is generated.

¹Department of Neurosurgery, Brigham and Women's Hospital, Mass General Brigham, Harvard Medical School, Boston, MA, USA. ²Department of Pathology, Brigham and Women's Hospital, Mass General Brigham, Harvard Medical School, Boston, MA, USA. ³Department of Biostatistics, Yale School of Public Health, New Haven, CT, USA. ⁴Department of Cancer Biology, Dana-Farber Cancer Institute, Harvard Medical School, Boston, MA, USA.

✉ e-mail: wbi@bwh.harvard.edu

Due to the lack of clarity regarding the minimum proportion of a chromosome arm that should be affected to consider it clinically meaningful, there is significant variability in the thresholds applied to generate chromosome arm calls across studies, ranging from 5 to 80%^{3,5,12}. Additionally, clinical cytogenetics laboratories often use an absolute segment size, as opposed to a percentage of the chromosome arm, to report segmental chromosome arm alterations¹³. The extent to which heterogeneity in thresholds affects the interpretation of molecular classification schemes remains unknown.

Given this variability, we investigated the distribution and prognostic impact of CNAs in a large clinically annotated cohort of meningiomas, the most common primary central nervous system tumor in adults¹⁴, for which robust CNAs have been shown to confer prognostic significance. For example, chromosome 1p loss has frequently been associated with malignant progression of meningiomas and thus has been integrated into several molecular classification schemes^{5,7,15}.

Here, we show the unique distribution of CNA gains and losses, as well as areas of CNA enrichment in the meningioma genome. We further explore CNA sizes in multifocal and primary-recurrent meningiomas, revealing the spatial and temporal dynamics of CNAs. Our findings demonstrate the value of defining arm call thresholds in meningioma molecular classification systems to allow reproducible genomic stratification across heterogeneous groups of patients.

Results

We profiled 1042 meningiomas using whole-genome microarrays and found that almost all cases (99.3%) had a detected CNA. As such, we surmised that the determination of whether a chromosome arm is considered lost or gained would be significantly influenced by the chosen size threshold. To investigate this, we evaluated two CNA arm call thresholds commonly reported in the literature, 5 and 50%, and observed a significant shift in the prevalence of arm losses and gains (Fig. 1A, B). There was a significant decrease in both arm loss calls (affecting 25 out of 39 arms tested, all $p < 0.05$) and arm gain calls (affecting 23 out of 39 arms tested, all $p < 0.05$).

Copy number alteration thresholds influence integrated grade assignment

To explore the cumulative effects of varying copy number calls as produced by different CNA arm call thresholds, we interrogated a copy number-driven molecularly Integrated Grade (IG). Molecular classification using IG has previously been shown to identify patients at risk for recurrence more accurately compared to the World Health Organization (WHO) grade, which stratifies meningiomas into 3 grades primarily using histopathologic features^{5,16}. This improvement in predictive performance through IG classification holds across all WHO grades. The IG is determined using several high-risk meningioma CNAs (loss of chromosome 1p, 3p, 4p/q, 6p/q, 10p/q, 14q, 18p/q, 19p/q), which have been shown to associate with recurrence risk across varying WHO grades and histopathological subtypes, along with *CDKN2A* loss status, and mitotic count. We assessed the assignment of IG classification while varying CNA arm call thresholds in meningiomas from 883 patients (68.2% WHO grade 1, 28.9% WHO grade 2, 2.9% WHO grade 3) with complete whole-genome microarray data, *CDKN2A/B* loss status, and recorded mitoses. As CNA arm call thresholds increased, meningiomas tended to shift to lower IG grades (Fig. 2A).

The distribution of low (IG-1) versus high (IG-2/3) grade meningiomas significantly differed at the upper and lower ends of CNA arm call thresholds. Applying a 5% CNA arm call threshold resulted in a significantly greater number of patients classified with an IG-2/3 meningioma compared to thresholds of 75% or 95% (both $p < 0.02$). The converse was observed with a 95% CNA arm call threshold, with a significantly smaller proportion of patients with an IG-2/3 meningioma compared to those at the 25, 50, and 75% thresholds (all $p < 0.01$). In total, 21.5% of patients shifted to a higher IG grade when moving from a 95% to 5% thresholds, with 14.3% of patients shifting from a low (IG-1) to high (IG-2/3) grade. Although meningioma IG designation did shift at the 25, 50, and 75% CNA arm call thresholds, the shifts were not statistically significant between these thresholds.

The chromosome arms contributing to the shift in IG grades across CNA arm call thresholds varied (Fig. 2B). From a 5% to 25% threshold, a reduction in 19q arm loss calls predominantly contributed to shifting patients to lower IG grades. 19p and 19q losses in particular

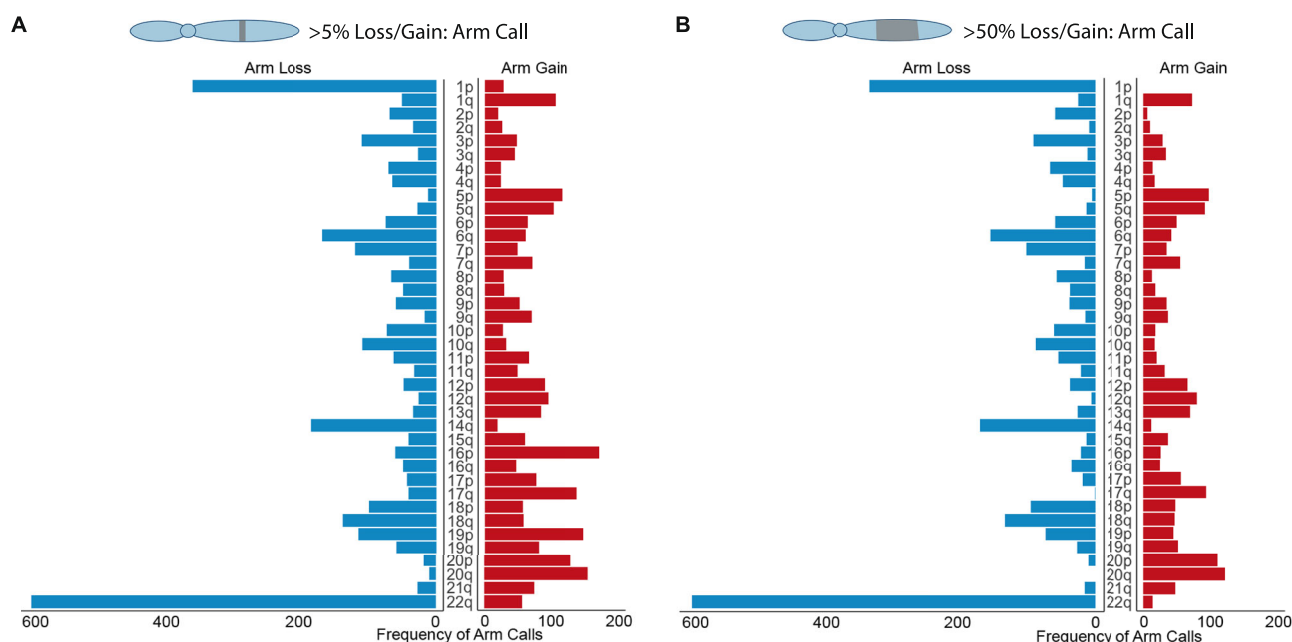


Fig. 1 | Chromosome arm calls across two arm call thresholds. A Frequency of chromosome arm gain and loss calls across the meningioma cohort ($n = 1042$) when a 5% arm call threshold is applied. **B** Frequency of gain and loss calls across the meningioma cohort ($n = 1042$) when a 50% arm call threshold is applied. Increasing

the arm call threshold decreased the frequency of gain and loss calls across a majority of chromosome arms (affected 25 of 39 arms tested for losses, 23 of 39 arms tested for gains, chi-squared test, two-sided, all $p < 0.05$). Source data are provided as a Source Data file.

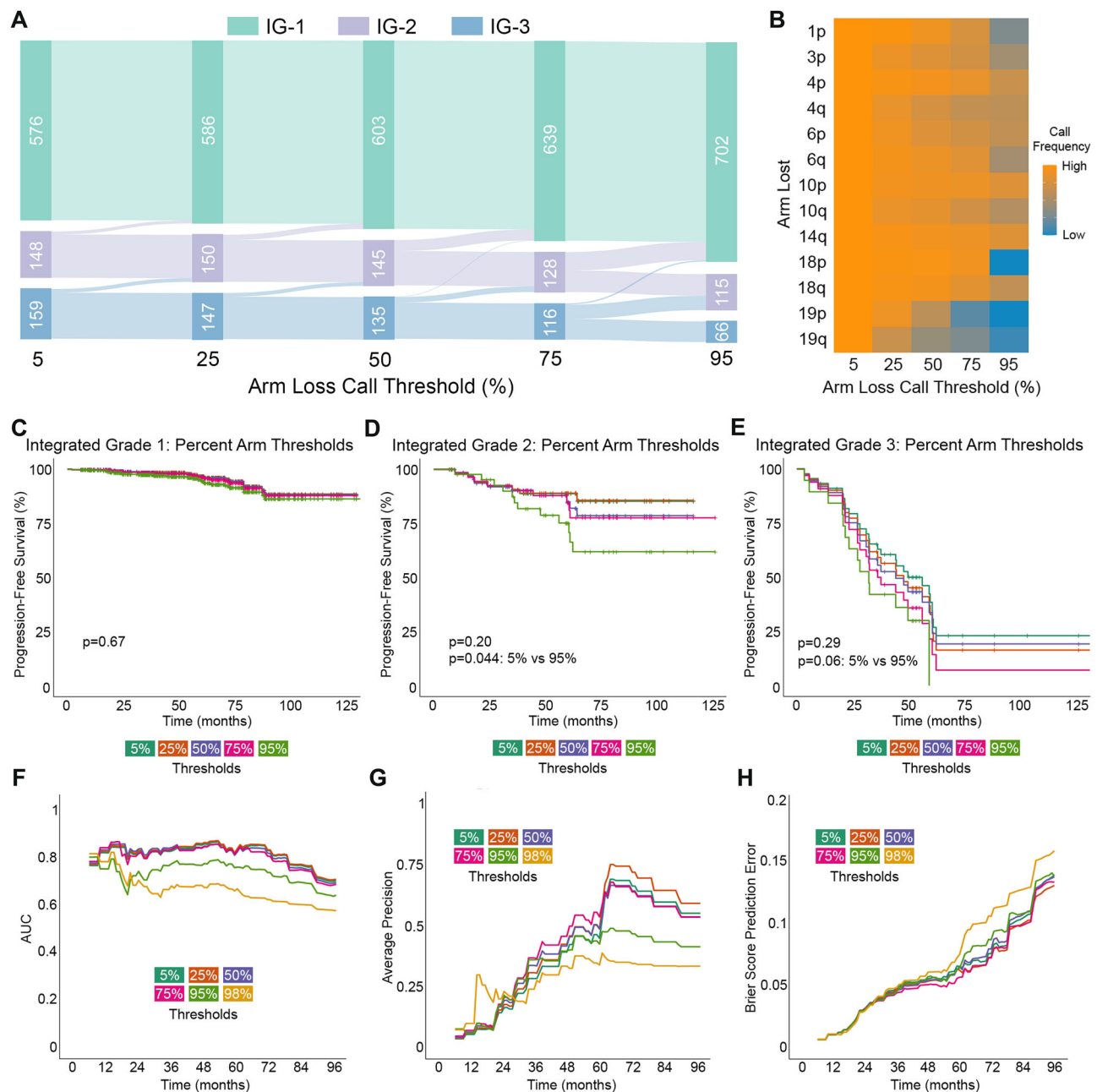


Fig. 2 | Impact of copy number thresholds on integrated grade. **A** Shifts in integrated grade (IG) classification for patients ($n = 883$) as CNA arm call thresholds were raised from 5% to 95%. **B** Heatmap of shifts in arm loss calls as CNA arm call thresholds were raised from 5% to 95%. Arms shown are part of the IG classifier for meningioma. Color scale shows frequency of [arm calls] from high (orange) to low (blue). Performance of IG classifier for predicting meningioma recurrence across different CNA arm call thresholds for IG-1 (**C**), IG-2 (**D**), and IG-3 (**E**) meningiomas

amongst patients with primary, gross-total resected meningioma with no prior radiation or chemotherapy and at least 6 months of follow-up ($n = 487$, log-rank test). Thresholds were varied as a percent of chromosome arm lost. Assessment of IG predictive capability for meningioma recurrence across selected CNA arm call thresholds using time-dependent receiver-operating curves (**F**), time-dependent average precision (**G**), and Brier scores for prediction error over time (**H**) across 487 patients. Source data are provided as a Source Data file.

showed a stepwise decrease in calls starting from the lowest arm call threshold. Other chromosome arms showed an incremental reduction over thresholds, such as 3p, while arms such as 18p significantly contributed to shifting IG grades only at the 95% threshold.

Copy number alteration thresholds and integrated grade recurrence prediction

The impact of CNA thresholds on predicting meningioma recurrence was most evident in aggressive meningiomas and at the extreme ends of the CNA threshold spectrum. Recurrence was examined in 487 patients with a primary, gross-total resected meningioma with no

prior radiation or chemotherapy and at least 6 months of follow-up (75.4% WHO grade 1, 23.8% WHO grade 2, 0.8% WHO grade 3). Patients were a median of 57 years old at surgery (range: 23–89 years), 72.6% were female, and 8.5% subsequently received adjuvant radiation. During the follow-up interval, 10.5% of patients had tumor recurrence (median follow-up: 4.7 years, range: 0.5–15 years).

Across all studied CNA arm call thresholds, there was no difference in progression-free survival (PFS: time to radiologically evident recurrence) for benign (IG-1) meningiomas, suggesting robustness of the IG-1 classification (Fig. 2C and Supplementary Fig. 1A, $p = 0.67$). This included when a “size-optimized” arm call threshold (Opt) was

tested: Opt was created by selecting different CNA arm call thresholds for each arm in the IG classifier, which maximized the arm's hazard ratio for meningioma recurrence. In meningiomas designated as IG-2, median PFS varied significantly between the 5% and 95% CNA call thresholds ($p = 0.044$, Fig. 2D and Supplementary Fig. 1C). PFS also varied between the 5% and Opt CNA call thresholds ($p = 0.026$). In the most molecularly aggressive meningiomas (IG-3), median PFS showed variation between the 5% and 95% thresholds but was not statistically significant (56.1 versus 32.2 months, respectively; Fig. 2E and Supplementary Fig. 1E, $p = 0.06$). PFS for the Opt threshold also diverged from the 5% threshold but was not statistically significant ($p = 0.11$). There was no significant difference in PFS between tumors classified at the 25, 50, and 75% CNA thresholds across IG-1, IG-2, and IG-3 meningiomas (Supplementary Fig. 1A, C, E). Amongst the patients who experienced a recurrence, when arm call thresholds were shifted from 95% to 5%, 19.6% were upgraded from low (IG-1) to high (IG-2/3) grade designation, which could potentially influence upfront clinical management.

Testing the capability of the IG classifier to predict recurrence across every CNA arm call threshold showed the best aggregate performance on time-dependent receiver operating curves when arm call thresholds were in the 38–42% range (Fig. 2F–H and Supplementary Fig. 2A–C). The highest CNA arm call thresholds (>95%) led to the worst prediction of meningioma recurrence, with a decrease in predictive performance starting even 1.5 years post-surgery. Brier scores over time, a measure of model accuracy and calibration, also reflected this, with increasing prediction error seen at thresholds restricting broad arm calls to whole arm CNA changes (thresholds >95%, Supplementary Fig. 2C). Time-dependent analysis of the Opt threshold did not significantly diverge from the performance of uniform CNA thresholds in the 38–42% range as well as the 50% threshold used to originally create the IG classifier (Supplementary Fig. 2A–C). However, consistent with previously reported data on the IG classifier defined at the 50% threshold, IG set at the Opt threshold outperformed the WHO grading criteria when predicting meningioma recurrence (Supplementary Fig. 3)⁵.

In practice, clinical cytogenetics labs report clinically significant chromosome arm alterations based on absolute size thresholds measured in megabases (Mb), rather than as a fraction of total chromosome length. For example, the clinical cytogenetics laboratory at Brigham and Women's Hospital uses 3 Mb of DNA as a threshold to define significant arm gains and losses. A clinically significant chromosome arm alteration could then be considered an arm gain or loss for use in a meningioma molecular classifier. Across all three IG grades, there was no significant difference in PFS between tumors classified with absolute CNA size thresholds between 3 and 15 Mb (Supplementary Fig. 1B, D, F).

Copy number alteration thresholds influence multiple independent meningioma classifiers

Beyond the IG classifier, CNA arm call thresholds impact risk stratification of additional independent molecular classifiers. These include the Integrated Score, which uses chromosome 1p, 6q, and 14q loss to stratify meningiomas into low, intermediate, and high risk of recurrence⁷, and the menG system, which applies multimodal molecular data, of which 1p and 22q loss form an integral component¹⁵. Applying the Integrated Score and menG systems to 883 patients demonstrated a shift toward lower grades as CNA arm call thresholds increased (Supplementary Fig. 4), similar to the phenomenon observed with CNA thresholds in IG. For the Integrated Score, applying a 5% CNA arm call threshold resulted in a significantly greater number of patients classified as intermediate or high risk of recurrence compared to thresholds of 75% or 95% (both $p < 0.01$, Supplementary Fig. 4A). In comparison, at the 95% threshold, significantly fewer patients were classified with intermediate or high risk meningiomas compared to those classified at the 25, 50, and 75 thresholds (all

$p < 0.001$). Meningioma Integrated Score designation also significantly shifted between a 25% versus a 75% threshold ($p = 0.005$). For the menG system, there was a significant difference in low- versus high-risk meningioma categorization between the highest threshold (95%) and all other tested thresholds ($p < 0.001$, Supplementary Fig. 4B).

Time-dependent prediction error analysis amongst the 487 patients with a primary, gross-total resected meningioma with no prior radiation or chemotherapy and at least 6 months of follow-up further validated the impact of varying CNA arm call thresholds using the Integrated Score classifier (Supplementary Fig. 5). The best aggregate performance of the Integrated Score on time-dependent receiver operating curves occurred at CNA thresholds between 46–48% (Supplementary Fig. 5A). Similar to the IG classifier, the Integrated Score showed decreasing receiver-operating curve and average precision values along with increased Brier prediction error scores when CNA arm call thresholds approached near-whole arm alterations (Supplementary Fig. 5A–C).

Meningioma copy number alterations demonstrate heterogeneity in size

We delved into the copy number landscape of the meningioma genome to understand how CNAs across chromosomes impact shifts in molecular classification. CNAs (1) involved one or both arms simultaneously, (2) were small or large in size, and (3) were either solitary (affecting one contiguous chromosome segment) or multiple (involving non-contiguous segments across a chromosome) (Fig. 3A). Specific chromosomes displayed preferential CNA patterns, with distinct involvement of the p arm (e.g., chr 1 losses), the q arm (e.g., chr 10 gains), or both the p and q arms (e.g., chr 18 gains). Additionally, copy number gains more frequently involved alterations present on both the p and q chromosome arms compared to CNA losses ($p < 0.05$).

Copy number gains and losses in meningioma genomes demonstrated a pattern of clustering into either small CNA segments ($\leq 10\%$ of chromosome length) or large CNA segments ($\geq 80\%$ of chromosome length), rather than a continuous distribution throughout the chromosome (Fig. 3B, C). Across gains and losses, 55.8% affected $\leq 10\%$ of the chromosome arm and 30.1% affected $\geq 80\%$, while only 14.1% affected between 10–90% of the arm (both $p < 0.001$, Fig. 4). Notably, the majority of CNAs manifested as a continuous solitary segment of the chromosome arm, with fewer than a quarter of events involving ≥ 2 fragments. A majority of copy number losses affected large segments of chromosome arms (median: 51.2% of the chromosome arm, average: 48.3%) (Fig. 4A, B).

On a megabase scale, copy number losses affected a median of 22.8 Mb (average: 34.1 Mb) and gains affected a median of 1.8 Mb (average: 17.2 Mb), with 64.4% of copy number losses and 38.0% of gains altering more than 3 Mb of a chromosome arm (Fig. 4C, D).

Meningioma copy number alterations show distinct localization

After filtering CNAs which are frequently observed in healthy patients¹⁷, meningioma copy number gains and losses showed differential frequency and location distributions across the genome (Fig. 5). Copy number losses were distributed across broad regions of the chromosome arm, with few discrete high-frequency CNA hotspots. Losses on many chromosome arms followed a similar pattern, with a greater frequency of meningiomas sustaining copy number losses toward the telomeres (e.g., chromosome 1p, 6q, 19p). An exception was chromosome 9p, which had an enrichment of copy number losses in a region including *CDKN2A/B* and *MTAP* (5.9% of meningiomas).

Copy number gains are also enriched in regions at both ends of the chromosome arms. Gains which enriched near the centromere included chromosome 1p (region with *NOTCH2*) in 5.4% of meningiomas and 22q (region with immunoglobulin lambda

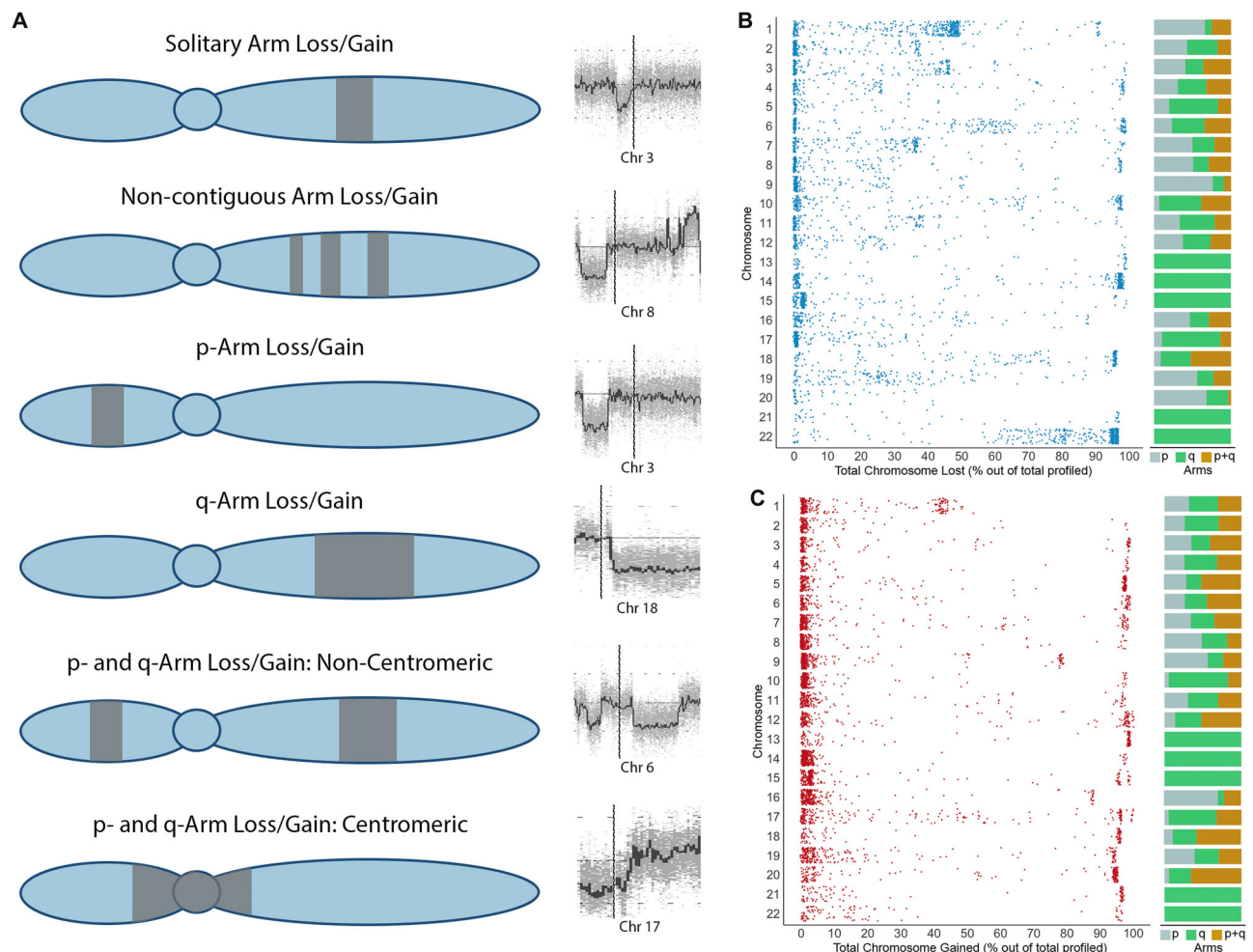


Fig. 3 | Copy number gains and losses in meningioma. A Phenotypes of copy number gains and losses across a chromosome with representative chromosome CNA plots. CNAs were (1) either solitary (affecting one contiguous chromosome segment) or non-contiguous (involving multiple non-contiguous segments across a chromosome) and (2) involved one arm or both arms simultaneously, with or

without centromeric involvement. Vertical line indicates centromere. **B** Size of copy number losses across the meningioma cohort ($n = 1042$) and affected chromosome arms. **C** Size of copy number gains across the meningioma cohort ($n = 1042$) and affected chromosome arms. Source data are provided as a Source Data file.

light chain locus, *MAPK1*) in 4.9% of meningiomas (Fig. 5). Gains toward the telomere included 5p (region with *TERT*) in 13.2% of meningiomas and 9q (region with *NOTCH1*) in 10.4% of meningiomas. However, some regions of high-frequency gains, such as that in the proximal segment of 14q (region with *TRAC*), likely represent normal polymorphisms driven by frequent segmental duplications^{18,19}.

Copy number alteration thresholds affect chromosome arm calls

We next sought to understand how CNA thresholds impact the designation of chromosome arm calls. By incrementally adjusting CNA arm call thresholds, we identified threshold ranges where arm calls exhibited significant variations. Determination of arm-level loss remained stable between CNA thresholds of 5–95% for most chromosome arms, while changing precipitously between thresholds of 0–5% and 95–100% (Fig. 6A and Supplementary Fig. 6A). However, a few arms—namely 17p, 19p, and 19q—showed a steady decline in chromosome arm loss calls as thresholds were increased between 5–95%. Similarly, for gains, most arm calls remained stable between 5–95% thresholds (Fig. 6B and Supplementary Fig. 6B). Arms 21q and 22q showed steady declines of chromosome arm gain calls up to a 15% threshold.

Optimal predictive copy number alteration thresholds are chromosome arm dependent

CNA arm call thresholds impacted the predictive value of chromosome arm calls for meningioma recurrence (Fig. 7). Recurrence was assessed in 487 patients who had a primary, gross-total resected meningioma without any prior radiation or chemotherapy and at least 6 months of follow-up. Out of the 39 arms tested for copy number losses, 30 arms were associated with meningioma recurrence at one or more CNA arm call thresholds on univariate testing. Across arms, the strength of association with meningioma recurrence varied as thresholds were altered. For instance, loss of chromosome 1p, the most commonly altered arm in aggressive meningiomas, showed increasing hazard ratios for recurrence as the CNA arm call threshold was raised toward 50% and declining hazard ratios at thresholds above 60–70%. By contrast, chromosome arms such as 6p had a stronger association with meningioma recurrence when nearly the entire arm was lost. This resulted in different “optimal” CNA call thresholds per arm: chromosome 1p loss demonstrated the highest hazard ratio for meningioma recurrence at a 46% CNA arm call threshold, while chromosome 18q loss showed the highest hazard ratio when an 87% CNA arm call threshold was applied (Supplementary Table 1). Compared to copy number losses, copy number gains were less often significantly associated with meningioma recurrence (Fig. 7B).

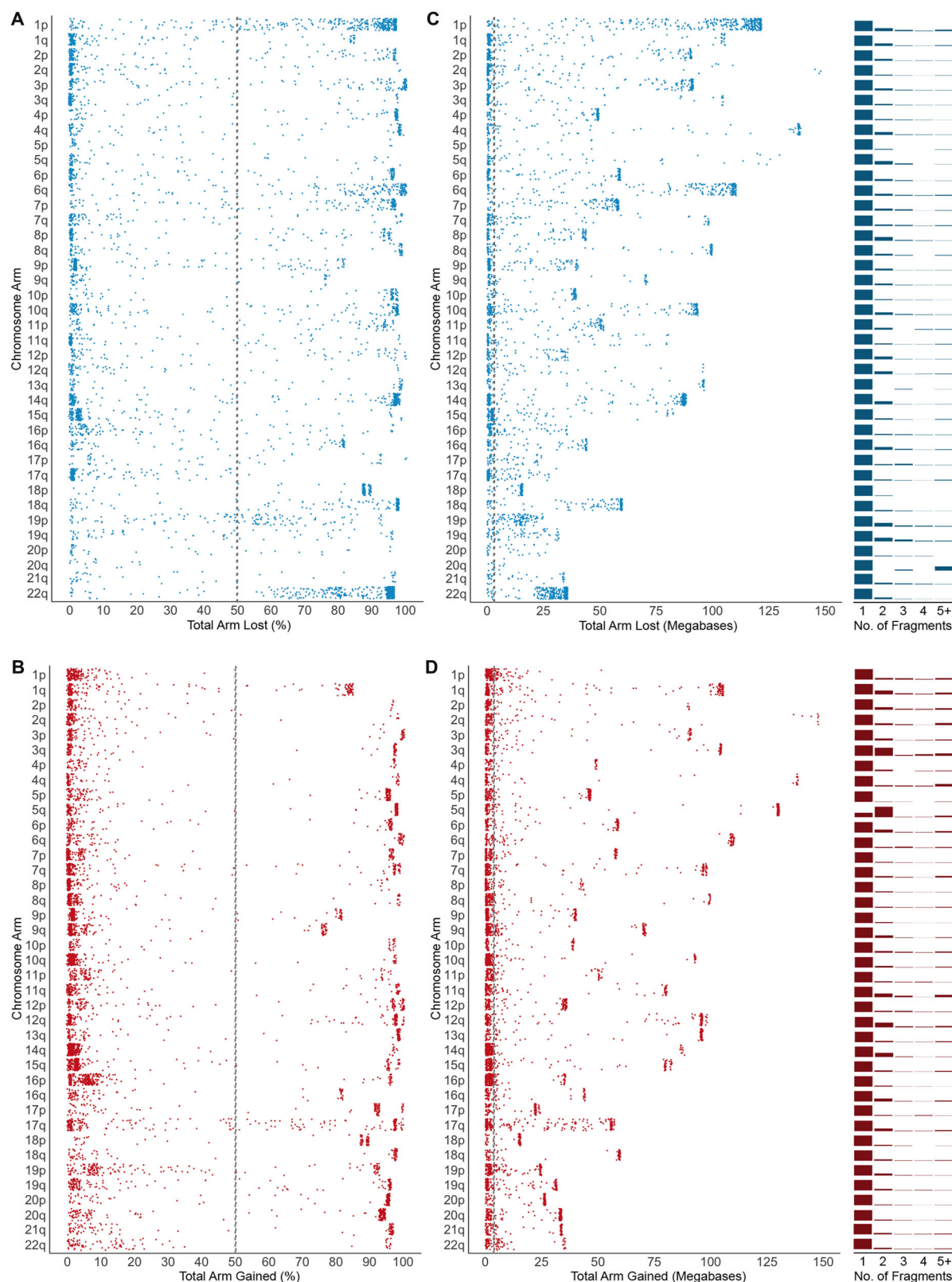


Fig. 4 | Distribution of meningioma copy number alterations. Size of copy number losses across the meningioma cohort ($n = 1042$) by chromosome arm as **A** percent of the chromosome arm or **C** as an absolute size of the chromosome arm in megabases. Number of fragments involved in chromosome arm losses. Size of

copy number gains across the meningioma cohort ($n = 1042$) by chromosome arm as **B** percent of the chromosome arm or **D** as an absolute size of the chromosome arm in megabases. Number of fragments involved in chromosome arm gains. Source data are provided as a Source Data file.

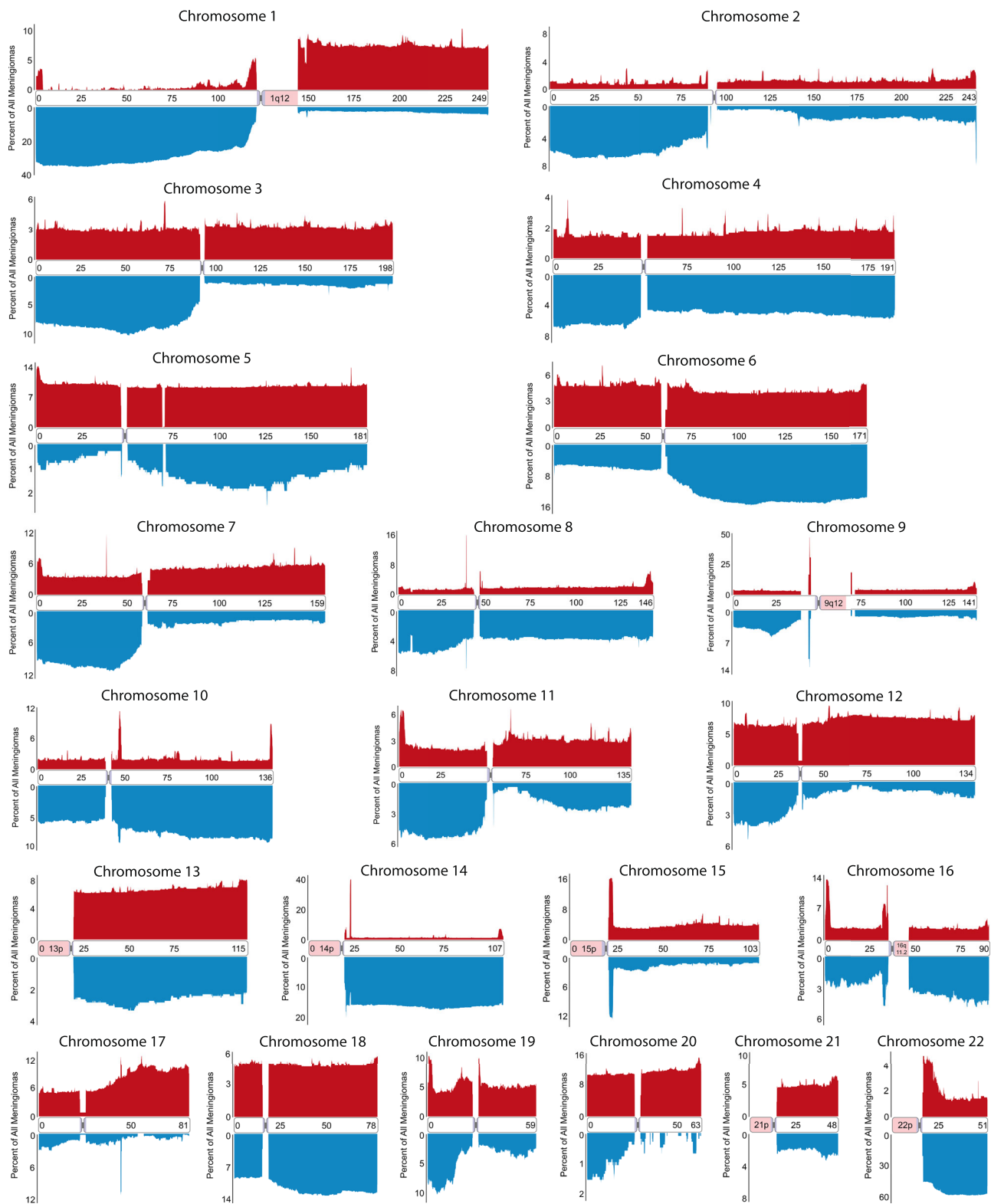


Fig. 5 | Location frequency maps of CNA gains and losses across the meningioma genome for the meningioma cohort ($n = 1042$). Plots below the x -axis (blue) are CNA losses, above the x -axis (red) are CNA gains. Source data are provided as a Source Data file.

Certain chromosome arms exhibited more variable association with meningioma recurrence across CNA arm call thresholds (Supplementary Fig. 7). To quantify this, a coefficient of variation (CV) was calculated using time-dependent receiver operating curves for

each chromosome arm across an 8-year follow-up window. Gains on 12 arms and losses on 11 arms showed the greatest predictive heterogeneity across thresholds, including arms such as 1p (loss), 1q (gain), and 22q (loss).

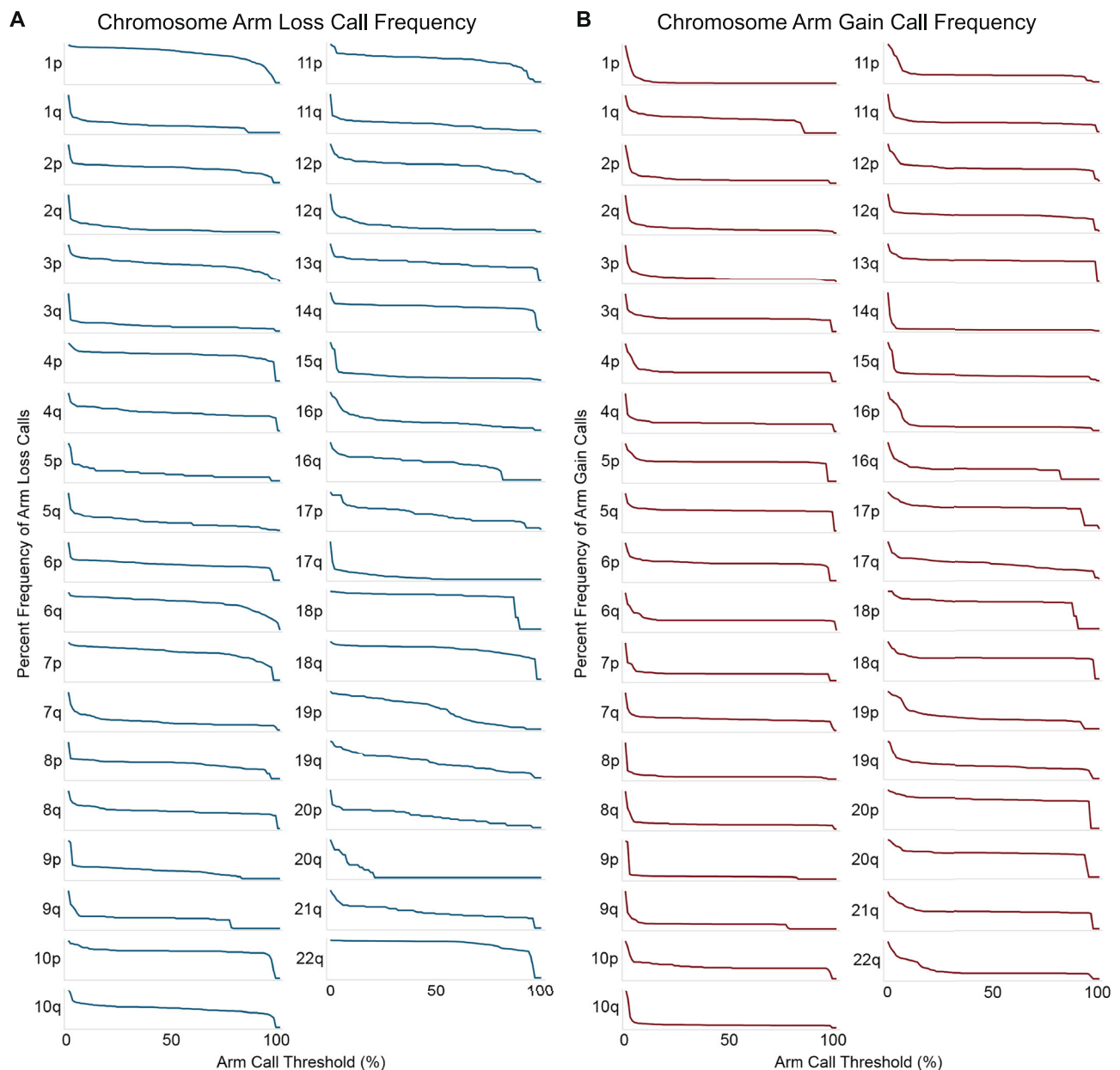


Fig. 6 | Change in chromosome arm call. Frequency of chromosome arm loss (A) and gain (B) calls as CNA arm call thresholds are varied from 0 to 100% across the meningioma cohort ($n = 1042$). Source data are provided as a Source Data file.

Chromosome 1p loss is clinically significant across copy number alteration thresholds

We specifically focused on 1p loss, the most common CNA in aggressive meningiomas, to further explore how varying CNA thresholds applied to an individual arm impact patient risk stratification. Chromosome 1p loss was significantly associated with meningioma recurrence at almost all CNA thresholds <98%, underscoring the clinical significance of small segmental 1p losses as prognostic markers for recurrence (Fig. 7A and Supplementary Table 1). Across CNA arm call thresholds between 5% and 95%, patients with chromosome 1p loss had significantly shorter median time to recurrence compared to those designated with WHO grade 1 (all $p < 0.001$, Supplementary Fig. 8). Meningiomas with 1p loss designated at the 50% and 75% thresholds were associated with significantly shorter median time to recurrence compared to those designated with WHO grade 2 meningiomas (both $p < 0.05$) while other 1p loss thresholds approached significance (5%: $p = 0.085$, 25%: $p = 0.079$, 95%: $p = 0.056$).

We also investigated smaller CNA losses (≤ 20 Mb) along chromosome 1 to determine if these alterations shed insight on focal chromosome regions that were prognostically significant. After dividing the total length of chromosome 1 into 10 Mb bins, we observed CNA losses on 1p between coordinates 90–100 Mb, 100–110 Mb, and 120–130 Mb as well as 1q losses between coordinates 140–150 Mb correlating with significantly shorter time to recurrence (all $p < 0.03$, Supplementary Fig. 9, chromosome 1 maximum length approximately 249 Mb). Small CNA losses in other regions across chromosome 1 did not significantly diverge in time to recurrence when compared to the cohort.

Copy number alteration sizes change incrementally in recurrent meningioma

Given the spectrum of CNAs associated with recurrence risk in meningioma, we explored how CNA sizes change as tumors evolve and whether the accumulation of CNAs contributes

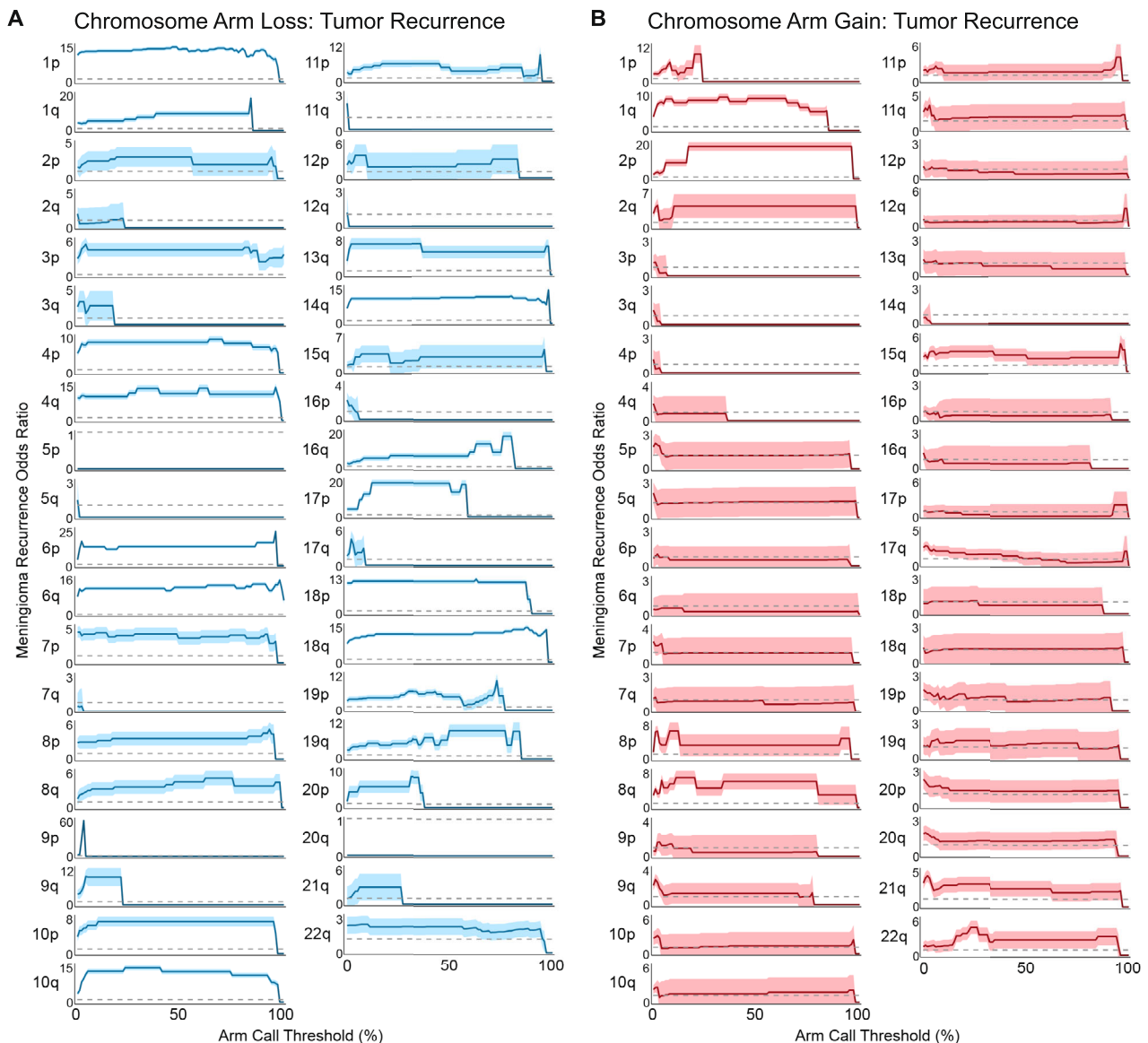


Fig. 7 | Copy number thresholds and recurrence risk. A, B Hazard ratios for meningioma recurrence per chromosome arm in 487 patients with primary, gross-total resected meningioma with no prior radiation or chemotherapy and at least 6 months of follow-up. Chromosome arm loss (**A**) and gain (**B**) calls were assessed as CNA arm call thresholds were varied from 0 to 100%. Data are presented as solid

blue or red line reflecting the hazard ratio for recurrence. Shaded blue or red regions are 95% confidence intervals for hazard ratios of recurrence. Dashed lines correspond to hazard ratio of 1, indicating a lack of association with recurrence. Source data are provided as a Source Data file.

to aggressive meningioma behavior. We examined CNAs in 13 patients with paired primary and recurrent meningiomas from serial resections. The median time between resections was 4.4 years: 30.8% of primary and 61.5% recurrent meningiomas were high-grade (grade 2 or 3) by WHO criteria. Using the IG system, 61.5% primary and 69.2% recurrent meningiomas were high-grade (IG-2, IG-3).

In 12 out of 13 patients, there was an increase in CNA size of $\geq 8\%$ on at least one altered chromosome arm between the primary and recurrent tumor (Fig. 8A and Supplementary Fig. 10). The size of the CNA change appeared to associate with meningioma grade. When examining the distribution of the largest CNA size change present for each patient, individuals with more aggressive primary/recurrent meningiomas (WHO grade 2/3) had a significantly greater CNA size change (mean: 86.8%) compared to those who had a primary WHO grade 1 meningioma which remained WHO grade 1 on recurrence (mean: 23.3%, $p = 0.015$).

Despite these large events, 40.6% of all CNAs remained stable in size upon recurrence while 29.4% of CNAs changed only slightly (1–5% of the chromosome arm length), predominantly showing growth in size (Supplementary Table 2). 30.0% of CNAs changed by $>5\%$ of the chromosome arm over time; within these, around half (52.3%) represented de-novo copy number changes in the recurrent tumor, which did not exist in the primary meningioma. This phenomenon likely reflects the cellular heterogeneity of meningioma and dynamic sub-clonal expansion and consolidation during tumor progression²⁰.

Analysis of paired primary and recurrent meningiomas in 3 patients as part of an external cohort demonstrated similar trends²¹. The median time between resections was 4 years, with primary tumors being WHO grade 1 ($n = 1$) or WHO grade 2 ($n = 2$). All three patients had an increase in CNA size of $\geq 37\%$ on at least one altered chromosome arm between primary and recurrent tumors. Similar to above, 34.1% of all CNAs remained stable in size upon recurrence, while 14.6% of CNAs changed only between 1–5% of the chromosome length. Of the 51.2% of

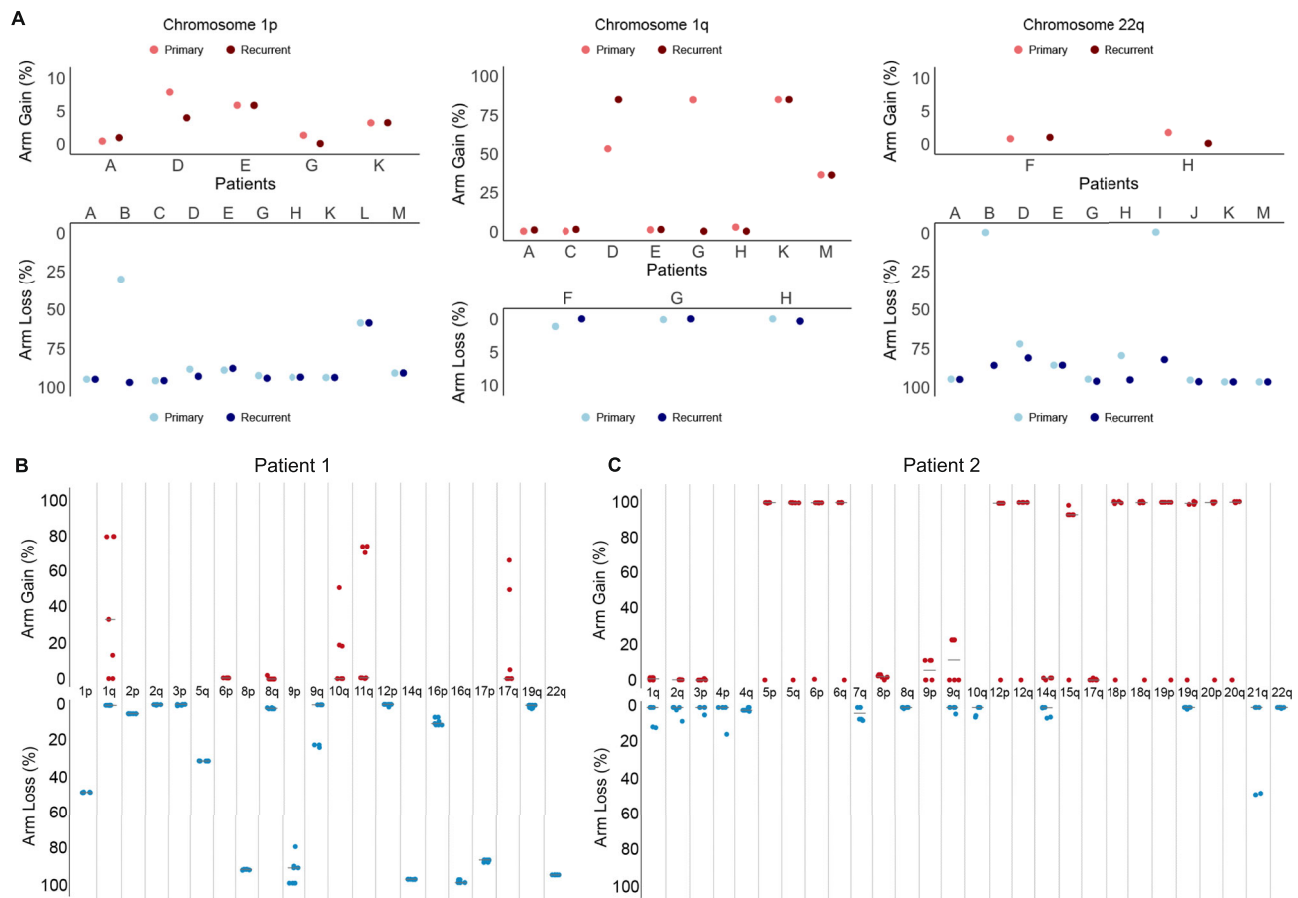


Fig. 8 | Copy number alterations in paired primary-recurrent and multifocal sampled meningiomas. **A** Copy number gains and losses from paired primary and recurrent meningiomas acquired from the same patient. Dots are paired for each patient, corresponding to their primary or recurrent tumor sample respectively. CNAs for chromosome arms 1p, 1q, and 22q shown here. **B, C** Gains and losses in

two patients with multifocal sampled meningioma. Each dot represents a different spatially distinct sample taken from a meningioma. Discrete clustering of CNA sizes across samples from the same tumor was seen across both losses (**B**) and gains (**C**). Source data are provided as a Source Data file.

CNAs which changed >5%, again, about half (57.1%) were de-novo CNAs that were not present in the primary tumor.

Copy number alteration sizes cluster in multifocal sampled meningiomas

We investigated whether CNAs manifest as distinct sizes across different regions within the same tumor by evaluating samples from 13 patients (median age: 65 years, female: 69.2%) who underwent multifocal sampling of their meningiomas (WHO grade 1 ($n = 7$), WHO grade 2 ($n = 3$), WHO grade 3 ($n = 3$), primary: 46.1%) with a median of 7 spatially distinct samples (range: 5–8)^{4,20}. While the pattern of chromosome CNAs varied across samples taken from the same meningioma, losses and gains within each affected chromosome in a given tumor were observed to cluster in two to three size groups rather than across a spectrum of different sizes (Fig. 8B, C and Supplementary Fig. 11).

Discussion

CNAs are frequently observed in meningioma genomes, carrying implications for tumor biology and clinical outcomes. As molecular classification paradigms develop that rely on chromosome arm calls generated from CNAs, it becomes crucial to understand how CNAs are distributed across the genome, how they evolve over space and time, and the consequences of the definitions used to convert CNAs to chromosome arm calls. With nearly a quarter of meningiomas shifting in IG classification across arm call thresholds, our analysis demonstrates critical considerations surrounding the utilization of these thresholds.

Meningioma CNAs primarily affected small (<10%) or large (>80%) amounts of the chromosome arm. Altering CNA thresholds resulted in a change in the frequency of arm calls in an arm-dependent manner. While we observed relative stability in the IG molecular classifier, which aggregates multiple chromosome arms, the differential effect of arm call thresholds is likely a factor influencing the stability of molecular classification schemes relying on chromosome arm calls. This threshold-dependent shift in molecular classification was further validated on application to two additional independent meningioma molecular classifiers, which also displayed variability when CNA thresholds were altered^{7,15}. As such, sensitivity testing across arm call thresholds can be a helpful step to ensure the reproducible translation of molecular classification schemes across institutions and patient populations.

The arm-dependent differences in CNA sizes and arm call thresholds affected the ability of arm calls to predict meningioma recurrence, with hazard ratios varying across arm call thresholds. Despite this, the IG meningioma classification scheme remained relatively stable in predicting meningioma recurrence, especially amongst IG-1 and IG-3 meningiomas, highlighting the strengths of this grading system. These groups reflect tumors with a rarer, small CNA changes or larger, more frequent CNA events, respectively, and therefore are less affected by varying CNA arm call thresholds. Absolute size-based thresholds (Mb) showed a similar effect, with no difference in time to recurrence for meningiomas classified as IG-1 or IG-3.

By contrast, performance across arm call thresholds for IG-2 meningiomas varied. These meningiomas represent a more

heterogenous group, which has proven challenging to categorize across histopathologic and molecular classification schemes^{3,22,23}. Some demonstrate aggressive, high-grade behavior while others remain more indolent, despite apparent similarities in pathological appearance or molecular composition. When a higher arm call threshold was applied (95%), this subset of meningiomas showed a shorter time to recurrence than IG-2 meningiomas identified at a lower arm call threshold (5%). This likely highlights the presence of a subset of IG-2 meningiomas with large CNA changes that behave more aggressively than IG-2 meningiomas with smaller CNA changes.

Assessing the predictive stability of the IG classifier across grades and timepoints showed a deterioration in performance when very high CNA arm call thresholds were applied. Even at shorter-term follow-up timepoints of 1 or 2 years, time-dependent receiver-operating curves showed notable decreased performance in predicting meningioma recurrence at thresholds above 80%. This drop in performance sustained over longer time horizons: up to 8 years in our analysis. Brier curves also reflected this, with very high CNA arm call thresholds showing consistently greater prediction error over time compared to lower CNA arm call thresholds. This pattern was consistent with the Integrated Score classifier as well. Therefore, restricting CNA arm calls to near whole-arm chromosomal alterations is likely not the best strategy to accurately capture patients at risk of meningioma recurrence over extended follow-up windows. Rather, for the IG classifier, if a single arm call threshold is required across all included chromosome arms, thresholds around 40% appear to maximize the predictive power of this classification scheme.

Analysis of multifocal sampled and primary-recurrent meningiomas supported geographic and temporal heterogeneity but also revealed discrete CNA size clusters, suggesting a predilection for CNA breakpoint sites across the genome²⁴. The consistency in CNA sizes across spatially distinct samples from the same meningioma demonstrates that, while there is intratumoral heterogeneity, CNAs are not steadily changing in size across subpopulations of tumor cells. Rather, there was greater variability in the collection of arms with CNAs in each sampled location. In paired primary-recurrent meningiomas, all patients had at least one significant chromosome CNA change in size, with more than half of these large CNA changes showing no alteration in the primary tumor. However, almost three-quarters of CNAs changed $\leq 5\%$ in size between primary and recurrent meningiomas in our internal cohort. This suggests that, amidst overall stability, there are occasional dynamic changes in the extent of CNAs in recurrent meningioma tumors, potentially linked to genomic instability that contributes to tumor recurrence.

Mapping the locations of meningioma CNAs revealed unique patterns in the distribution of gains and losses. For several high-risk chromosome arms such as 1p, 6p, and 10q, copy number losses appeared to enrich near the telomeres. This result is consistent with findings from other cancer types, where broad CNA losses frequently start near the telomeres—among the most gene rich regions of the genome—but are more variable in their length of extension across the chromosome arm²⁴. Yet certain chromosome arms, such as 9p and 19q did show a higher frequency of losses in interstitial segments, potentially indicating discrete regions of the meningioma genome under selection. Through smaller CNA losses on chromosome 1, we began to see how specific chromosome regions associate with recurrence risk, indicating that there may be specific loci amongst larger CNA changes conferring a cellular survival advantage or disadvantage. Copy number gains did show some more focal hotspots, notably around the pericentromeres and near the telomeres, such as on 1p and 5p. Of note, we observed a high frequency of CNAs in focal regions such as T-cell receptor clusters, which were filtered from the meningioma genome after comparison to CNAs found in the normal population. This underscores the background population-level variability of CNAs and the complexity of isolating and assessing the clinical significance of CNAs linked to meningioma evolution.

The framework presented here demonstrates how CNAs and their translation into molecular classification schemes can be systematically investigated. However, this study does have certain limitations, many of which are associated with the modalities used for genomic profiling. While we can identify CNAs through whole-genome microarray and DNA methylation data, drawing definitive conclusions on the role of specific CNA loci and how these CNAs impact gene expression is challenging. Combining this data with RNA sequencing or proteomics might help determine the biological consequences of CNAs enriched in particular locations. Additionally, our primary cohort was limited to cases evaluated at a single institution. While we incorporated publicly available meningioma data to capture the heterogeneity in tumor molecular alterations, findings on the spatial distribution of CNAs as well as primary-recurrent tumor pairs require a larger investigation with greater power. Collectively, our analysis demonstrates a pathway for understanding and integrating CNAs into meningioma molecular classification systems, a step toward improving prognostic models and identifying the downstream implications of CNAs.

Methods

Patient cohort

We assembled a cohort of patients with meningioma evaluated at Brigham and Women's Hospital (BWH) with resection performed between 2007–2021. Patients were selected if whole-genome microarray data were available from our institutional clinical cytogenetics laboratory. Demographic information such as age and self-reported sex, clinical history, and follow-up information on overall survival (OS) was extracted from the electronic medical record. Meningioma histopathologic grade was extracted from pathology reports, with histopathologic grade assigned by neuropathologists using the 2007 and 2016 WHO classification guidelines^{16,25}. WHO guidelines divide meningiomas into three grades: grade 1 (more benign), grade 2 (intermediate), and grade 3 (more aggressive). Diagnostic criteria for each WHO grade reflect the rate of mitoses, tissue features such as necrosis or hypercellularity, and tumor characteristics such as brain invasion. Mitotic count per 10 high-powered fields was also extracted from the clinical record. This study was approved by the Institutional Review Board at BWH/Dana-Farber Cancer Center, with a waiver of written or signed patient consent. A waiver for informed consent was granted due to the retrospective nature of the dataset utilizing existing medical records, with no publicly reported identifiable information. Additional grounds for waiving informed consent included the number of subjects encompassed, resource burden in locating individuals, and patient selection bias if informed consent were required. The rights and welfare of patients were deemed not to be adversely affected in retrospective data collection included as part of this study. No compensation was provided to participants.

Progression-free survival (PFS) was defined as time to radiologically evident first recurrence of meningioma. Follow-up MRI images were reviewed independently by neurosurgeons and neuroradiologists to evaluate for recurrence. Gross-total resection was defined after volumetric post-operative image contouring, which demonstrated no residual tumor²⁶. Paired primary-recurrent samples were identified if molecular profiling was performed on a patient's primary and recurrent meningioma. This study was approved by the Institutional Review Board at BWH.

Chromosome copy number analysis

Chromosome copy number was assessed using the Affymetrix OncoScan assay, a whole genome single-nucleotide polymorphism (SNP) based microarray with 217,611 probes and an average resolution of approximately 300 kilobases²⁷. Chromosome Analysis Suite Software (ThermoFisher Scientific) was used to perform an *in silico* comparison between the hybridization pattern of a patient specimen against a pooled reference sample set.

Segmented microarray data for each meningioma samples was processed using probe start and end locations to determine the size of CNAs in DNA base pairs. GRCh37/hg19 was used for probe localization and subsequent chromosome arm calculations. CNAs present in healthy control populations were filtered out using a validated consensus stringent CNA map¹⁷. The size of each CNA was divided by the total profiled chromosome size and chromosome arm size to determine the percent of the total chromosome affected and percent of the chromosome arm affected. If multiple CNAs of the same type (e.g., loss or gain) occurred on the same chromosome arm for a given sample, fragment sizes were combined. Differences in CNA sizes were statistically compared using the Wilcoxon rank-sum test at a significance level of $p < 0.05$.

The locations of CNAs across the entire sample set were compiled, generating location CNA frequency maps of the meningioma genome. For each arm, a baseline arm CNA value was established using the median number of meningiomas with a CNA affecting a given arm. Location peaks in CNA were defined as any discrete clusters across a chromosome arm exceeding one and a half times the baseline arm CNA value. The NCBI Genome Data Viewer (assembly GRCh37/hg19) was then used to identify genes in each location peak.

To understand how chromosome arm CNA thresholds impact chromosome arm calls, thresholds were incremented between 0–100% at 1% increments. The change in chromosome arm call frequency was plotted separately for CNA gains and losses across each chromosome arm. The first derivative of each plot was taken to determine thresholds which result in the greatest change of chromosome arm calls.

CNA arm loss calls, *CDKN2A* loss status, and mitotic count were used to calculate a Molecularly Integrated Grade (IG) for meningioma⁵. IG was calculated at various chromosomal arm loss thresholds. CNA arm loss calls were also utilized to test two additional meningioma molecular classifiers, the Integrated Score and the CNA component of the menG system^{7,15}. Differences in low (IG-1, Int-Score low, menG A) versus high (IG-2/3, Int-Score intermediate/high, menG B/C) grade categorization across chromosome arm loss thresholds were evaluated using Chi-squared with Bonferroni adjustment at a significance level of $p < 0.05$.

Primary-recurrent and multifocal sampled meningioma

Using two publicly available datasets generated at the University of California, San Francisco (UCSF), we assessed chromosome copy number profiles in patients who had paired primary-recurrent meningiomas, as well as with multiple stereotactic samples collected for each meningioma^{4,21}. DNA was extracted from each sample and processed on the Illumina Methylation EPIC Beadchip. GRCh37/hg19 was used for probe localization. CNA profiles were generated from this DNA methylation data using the *conumee* package in R, using whole blood methylation profile data as a copy number normal control²⁸. CNA intensity value distributions were then processed according to previously published mean segment intensities: segments with a mean intensity value of less than -0.1 were defined as copy number losses, and segments with a mean intensity value of greater than 0.15 were defined as copy number gains³.

The size of each CNA segment, determined using the probe start and end location, was used to calculate the percent of the chromosome arm affected by each CNA. For paired primary-recurrent tumors, the change in CNA size was computed between each sample pair. For multifocal sampled tumors, CNA profiles derived from the same meningioma sample were plotted together to assess spatial variability in CNA size.

Integrated grade and progression-free survival

The impact of chromosome arm call thresholds on predicting PFS was examined in patients with primary meningiomas who had no prior radiation or chemotherapy treatment, and if gross-total resection was achieved. Patients were included if at least 6 months of follow-up data

were available. CNA calls were computed at each threshold from 0–100% in increments of 1%. At each threshold, a logistic regression model was fit to chromosome arm calls and meningioma recurrence data, generating an odds ratio for recurrence at each chromosome arm call threshold. Odds ratios, along with 95% confidence intervals, were plotted across arm call thresholds. Odds ratios at the point of collinearity, when infinitely large or small due to complete positive or negative correlation, were excluded.

Kaplan–Meier curves were generated across selected chromosome arm call thresholds to determine how the IG classification system differences in predicting meningioma recurrence across thresholds. Five arm call thresholds were selected based on the percentage of an arm lost: 5%, 25%, 50%, 75%, 95%. Five arm call thresholds were also assessed based on the absolute size of an arm lost in megabases (Mb): 3 Mb, 6 Mb, 9 Mb, 12 Mb, and 15 Mb. An optimized arm call threshold was also tested (Opt). The Opt threshold was developed by assigning an arm-dependent threshold value, selected based on the value that resulted in the highest hazard ratio for meningioma recurrence on univariate logistic regression. Kaplan–Meier curves for meningioma PFS across various thresholds were compared within each IG using the log-rank test, with curves significantly different at $p < 0.05$.

The capability of the IG classification system to predict meningioma recurrence was examined across all CNA arm call thresholds using time-dependent receiver operating curves, time-dependent average precision (a measure of model consistency), and Brier scores over time (a measure of model accuracy and calibration for predictions). Cox models were fitted for Brier score computation. Time-dependent analysis was also performed to assess the Integrated Score classification system. Time-dependent receiver operating curves were further used to compute a coefficient of variation (CV) for the association between a chromosome arm and meningioma recurrence across CNA thresholds. CV values were used to determine which chromosome arms were most sensitive to changes in CNA thresholds in the context of meningioma recurrence. The time window was captured from 6 months to 8 years, and all analyses were performed in R (*timeROC*, *APsurv*, *brier*).

Reporting summary

Further information on research design is available in the Nature Portfolio Reporting Summary linked to this article.

Data availability

The whole-genome meningioma microarray data included in this study have been deposited in the Gene Expression Omnibus (GEO) database under accession codes [GSE287920](#) and [GSE287929](#). Publicly available DNA methylation data on paired primary-recurrent and multifocal sampled meningiomas can be found at [GSE228316](#) and [GSE151067](#). Source data are provided with this paper.

Code availability

Packages “minfi”, “conumee”, and “IlluminaHumanMethylationEPICanno.ilm10b4.hg19” from Bioconductor were used as part of this manuscript for methylation analyses. Bioconductor packages have open-source licenses. No other custom code was utilized. All analyses were performed in R with open-source packages and tools detailed in the methods section. R scripts used for analysis and figure generation are available on GitHub [https://github.com/ruchit317/Meningioma_CNA] under an open-source MIT License.

References

- Golub, T. R. et al. Molecular classification of cancer: class discovery and class prediction by gene expression monitoring. *Science* **286**, 531–537 (1999).
- Nassiri, F. et al. A clinically applicable integrative molecular classification of meningiomas. *Nature* **597**, 119–125 (2021).

3. Choudhury, A. et al. Meningioma DNA methylation groups identify biological drivers and therapeutic vulnerabilities. *Nat. Genet.* **54**, 649–659 (2022).
4. Magill, S. T. et al. Multiplatform genomic profiling and magnetic resonance imaging identify mechanisms underlying intratumor heterogeneity in meningioma. *Nat. Commun.* **11**, 4803 (2020).
5. Driver, J. et al. A molecularly integrated grade for meningioma. *Neuro Oncol.* **24**, 796–808 (2022).
6. Sahm, F. et al. DNA methylation-based classification and grading system for meningioma: a multicentre, retrospective analysis. *Lancet Oncol.* **18**, 682–694 (2017).
7. Maas, S. L. N. et al. Integrated molecular-morphologic meningioma classification: a multicenter retrospective analysis, retrospectively and prospectively validated. *J. Clin. Oncol.* **39**, 3839–3852 (2021).
8. Steele, C. D. et al. Signatures of copy number alterations in human cancer. *Nature* **606**, 984–991 (2022).
9. Beroukhi, R. et al. The landscape of somatic copy-number alteration across human cancers. *Nature* **463**, 899–905 (2010).
10. Bi, W. L. et al. Genomic landscape of high-grade meningiomas. *NPJ Genom. Med.* **2**, 15 (2017).
11. Zack, T. I. et al. Pan-cancer patterns of somatic copy number alteration. *Nat. Genet.* **45**, 1134–1140 (2013).
12. Hielscher, T. et al. Clinical implementation of integrated molecular-morphologic risk prediction for meningioma. *Brain Pathol.* **33**, e13132 (2023).
13. Neveling, K. et al. Next-generation cytogenetics: comprehensive assessment of 52 hematological malignancy genomes by optical genome mapping. *Am. J. Hum. Genet.* **108**, 1423–1435 (2021).
14. Ostrom, Q. T., Cioffi, G., Waite, K., Kruchko, C. & Barnholtz-Sloan, J. S. CBTRUS statistical report: primary brain and other central nervous system tumors diagnosed in the United States in 2014–2018. *Neuro Oncol.* **23**, iii1–iii105 (2021).
15. Bayley, J. C. et al. Multiple approaches converge on three biological subtypes of meningioma and extract new insights from published studies. *Sci. Adv.* **8**, eabm6247 (2022).
16. Louis, D. N. et al. The 2016 World Health Organization classification of tumors of the central nervous system: a summary. *Acta Neuropathol.* **131**, 803–820 (2016).
17. Zarrei, M., MacDonald, J. R., Merico, D. & Scherer, S. W. A copy number variation map of the human genome. *Nat. Rev. Genet.* **16**, 172–183 (2015).
18. Young, J. M. et al. Extensive copy-number variation of the human olfactory receptor gene family. *Am. J. Hum. Genet.* **83**, 228–242 (2008).
19. Iben, J. R. & Maraia, R. J. tRNA gene copy number variation in humans. *Gene* **536**, 376–384 (2014).
20. Vasudevan, H. N. et al. Intratumor and informatic heterogeneity influence meningioma molecular classification. *Acta Neuropathol.* **144**, 579–583 (2022).
21. Lucas, C.-H. G. et al. Spatial genomic, biochemical and cellular mechanisms underlying meningioma heterogeneity and evolution. *Nat. Genet.* <https://doi.org/10.1038/s41588-024-01747-1> (2024).
22. Aghi, M. K. et al. Long-term recurrence rates of atypical meningiomas after gross total resection with or without postoperative adjuvant radiation. *Neurosurgery* **64**, 56–60 (2009).
23. Aizer, A. A. et al. Extent of resection and overall survival for patients with atypical and malignant meningioma. *Cancer* **121**, 4376–4381 (2015).
24. Shih, J. et al. Cancer aneuploidies are shaped primarily by effects on tumour fitness. *Nature* **619**, 793–800 (2023).
25. Louis, D. N. et al. The 2007 WHO Classification of tumours of the central nervous system. *Acta Neuropathol.* **114**, 97–109 (2007).
26. Huang, R. Y. et al. Proposed response assessment and endpoints for meningioma clinical trials: report from the Response Assessment in Neuro-Oncology Working Group. *Neuro Oncol.* **21**, 26–36 (2019).
27. Craig, J. M. et al. DNA fragmentation simulation method (FSM) and fragment size matching improve aCGH performance of FFPE tissues. *PLoS ONE* **7**, e38881 (2012).
28. Owen, B. M., Phie, J., Huynh, J., Needham, S. & Fraser, C. Evaluation of quantitative biomarkers of aging in human PBMCs. *Front. Aging* **4**, 1260502 (2023).

Acknowledgements

This study was supported by the Courtney Meningioma Research Fund (W.L.B.) and Fleming Meningioma Research Fund (W.L.B.).

Author contributions

Study conception and design: R.V.P. and W.L.B. Development of methodology: R.V.P., H.S.G., D.M., and W.L.B. Data acquisition, analysis, interpretation, visualization: R.V.P., H.S.G., D.M., S.R., E.B.C., R.B., A.H.L., S.S., and W.L.B. Manuscript production: R.V.P., H.S.G., D.M., S.R., E.B.C., R.B., A.H.L., S.S., and W.L.B. All authors had full access to the data included in this manuscript and approved submission.

Competing interests

The authors declare no competing interests.

Additional information

Supplementary information The online version contains supplementary material available at <https://doi.org/10.1038/s41467-025-60734-0>.

Correspondence and requests for materials should be addressed to Wenya Linda Bi.

Peer review information *Nature Communications* thanks Ana Valeria Castro and Andrew Lynch for their contribution to the peer review of this work. A peer review file is available.

Reprints and permissions information is available at <http://www.nature.com/reprints>

Publisher's note Springer Nature remains neutral with regard to jurisdictional claims in published maps and institutional affiliations.

Open Access This article is licensed under a Creative Commons Attribution-NonCommercial-NoDerivatives 4.0 International License, which permits any non-commercial use, sharing, distribution and reproduction in any medium or format, as long as you give appropriate credit to the original author(s) and the source, provide a link to the Creative Commons licence, and indicate if you modified the licensed material. You do not have permission under this licence to share adapted material derived from this article or parts of it. The images or other third party material in this article are included in the article's Creative Commons licence, unless indicated otherwise in a credit line to the material. If material is not included in the article's Creative Commons licence and your intended use is not permitted by statutory regulation or exceeds the permitted use, you will need to obtain permission directly from the copyright holder. To view a copy of this licence, visit <http://creativecommons.org/licenses/by-nc-nd/4.0/>.

© The Author(s) 2025